

VHE emission from M 82

Massimo Persic¹, Yoel Rephaeli^{2,3}, and Yinon Arieli^{2,3}

¹ INAF/Osservatorio Astronomico di Trieste and INFN-Trieste, via G.B. Tiepolo 11, 34143 Trieste, Italy

² School of Physics & Astronomy, Tel Aviv University, Tel Aviv 69978, Israel

³ Center for Astrophysics and Space Sciences, University of California at San Diego, La Jolla, CA 92093, USA

Received; accepted

Abstract.

Spurred by the improved measurement sensitivity in the very-high-energy (VHE) γ -ray (≥ 100 GeV) band, we assess the feasibility of detection of the nearby starburst galaxy M 82. TeV emission is expected to be predominantly from the decay of neutral pions which are produced in energetic proton interactions with ambient protons. An estimate of TeV emission from this process is obtained by an approximate, semi-quantitative calculation, and also by a detailed numerical treatment based on a convection-diffusion model for energetic electron and proton propagation and energy losses. All relevant hadronic and leptonic processes are considered, gauged by the measured synchrotron radio emission from the inner disk region. We estimate an integrated flux $f(\geq 100 \text{ GeV}) \sim 3 \times 10^{-12} \text{ cm}^{-2} \text{ s}^{-1}$. This level of TeV emission puts M 82 within reach of the upcoming enhanced imaging air Cherenkov telescopes, such as MAGIC II.

Key words. Galaxies: cosmic rays – Galaxies: gamma-ray – Galaxies: spiral – Galaxies: star formation

1. Introduction

In the central regions of starburst galaxies (SBGs) high level of star formation (SF) activity powers the emission of radiation directly by supernovae (SN) of massive stars, and indirectly by SN shock heating of interstellar gas and dust, as well as from radiative processes involving electrons and protons that are accelerated by SN shocks. Kinetic energy of the non-thermally distributed electrons and protons is partly channeled into radio to the high-energy γ -ray emission. In particular, radiation in the TeV region is emitted predominantly in π^0 decay, following the production of the pions in energetic proton interactions with protons in the gas, and by relativistic electrons traversing (relatively) strong magnetic field and scattering off the intense radiation field in the galactic disk.

The level of high-energy phenomena in intensely active galaxies makes AGN obvious targets of searches for TeV emission, and indeed some 15 blazars have already been detected by H.E.S.S. and MAGIC (e.g., Persic & De Angelis 2008). Various issues in the study of non-thermal phenomena in ‘normal’ and starburst galaxies are no less interesting and important. Valuable insight can be gained on the origin and propagation modes of relativistic electrons and protons by probing their radiation yields across the electromagnetic spectrum. Knowledge of the low energy densities of these particles is important also for quantifying their impact on interstellar gas.

At a distance $d=3.6$ Mpc (Freedman et al. 1994), the SB galaxy M 82 is a good candidate for an initial search for

TeV emission from a galaxy whose emission is not AGN-dominated. Its far-infrared and X-ray luminosities imply high SF rates (e.g., Persic & Rephaeli 2007), and a correspondingly high SN rate of 0.3 yr^{-1} (Rieke et al. 1980). In most respects, levels of activity in M 82 surpass those in the other nearby starburst galaxy, NGC 253, making it a very good target for TeV observations, also in view of its large reservoir of diffuse gas ($\sim 10^9 M_{\odot}$; Casasola et al. 2004).

In order to realistically estimate non-thermal emission from cosmic-ray electrons and protons, we start with the initial spectrum that characterizes their momentum distribution at the acceleration sites, and follow the evolution of the spectrum as the particles diffuse and are convected from the inner SB region to the outer disk (and halo). All the relevant leptonic and hadronic interactions are included in a numerical program we have developed for this purpose. Using this program we can determine the particle spatial and energy distributions, and their respective radiative yield across the galaxy. For a more intuitive approach, and in order to compare with previous semi-quantitative estimates, we also use a simple analytical model of the diffuse hadronic emission of M 82, that ties the predicted γ -ray flux to the measured on-site synchrotron radio flux by assuming energetic particles and magnetic field to be in energy equipartition.

In Section 2 we briefly review the basic features of predicted particle source spectra, the relation between the cosmic-ray electron and proton components, and key aspects of their energy-loss processes and propagation in galaxies. We then summarize the main features of our numerical program which

is used to determine the particle spectro-spatial distribution. In Section 3 we present a specific estimate of the hadronic emission from M 82 based on our approximate analytical treatment. Results of our detailed numerical analysis are presented in Section 4, and discussed in Section 5.

2. Particle Spectra and Energy Loss Processes

2.1. Particle Source Spectra

SN shock wave sweeps and compresses circumstellar material with a compression ratio $s \equiv (\gamma_c + 1)/[\gamma_c - 1 + 2(\beta/M)^2]$, where $\gamma_c \equiv C_P/C_V = 5/3$ is the specific heat ratio, $\beta \equiv (c_s/V_A)$ is the speed of sound (c_s) in units of the Alfvén velocity (V_A), and $M \equiv u_1/V_A$ is the Alfvénic Mach number of the shock, with u_1 denoting the upstream velocity of the gas. Particle acceleration by the shock modifies the momentum distribution to a power-law whose index depends on M . When particles with initial momentum p_0 are overtaken by the shock, the resulting downstream phase space distribution function is $f(p) \propto p^{-\eta}$ (for $p > p_0$) where $\eta = 3s/(s-1) = 3M^2(\gamma+1)/2(M^2-1)$ (Blandford & Ostriker 1978). The number density of accelerated particles per momentum interval dp is $N(p) \propto f(p)p^2 \propto p^{-q}$ with $q = \eta - 2$, and it can be readily seen (from conservation of particle number) that the particle density per unit energy interval, $N(E)$, has the same index q , $N(E) \propto E^{-q}$. In the strong shock limit, $\eta=4$, so $q=2$, a well-known result for the first-order Fermi acceleration mechanism (e.g. Protheroe & Clay 2004). Particles are accelerated to very high energy ($E \geq 10^{14}$ eV). The steepening of their power-law distribution (due to energy losses outside the source region) implies that – for our purposes here – the specific value of the high energy cutoff is irrelevant. On the other hand, the lower energy cutoff has practical relevance; acceleration models predict a minimum kinetic energy $T_{e,\min} \sim 10$ keV.

If electrons and protons are accelerated such that they have the same differential power-law momentum spectrum, $N_i(p) = N_{i,0} p^{-q}$, with $i = e, p$ (subscript p stands for proton, not momentum), then their respective densities (or energy densities) can be readily related – in the source region – when requiring charge neutrality to be maintained for the accelerated ($T \geq T_0 = 10$ keV) particles (and not just for the gas reservoir from which they originate). As function of kinetic energy $T = (\gamma - 1)mc^2$, where γ is the particle Lorentz factor, the p/e number density ratio is (e.g., Schlickeiser 2002),

$$\frac{N_p(T)}{N_e(T)} \simeq \left(\frac{m_p}{m_e}\right)^{(q-1)/2} \left(\frac{T + m_p c^2}{T + m_e c^2}\right)^{-(q-1)/2}, \quad (1)$$

where m_e and m_p are the electron and proton masses. This ratio assumes the following limiting forms

$$\frac{N_p(T)}{N_e(T)} \simeq \begin{cases} 1 & T \ll m_e c^2; \\ [T/(m_e c^2)]^{\frac{q-1}{2}} & m_e c^2 \ll T \ll m_p c^2; \\ \left(\frac{m_p}{m_e}\right)^{\frac{q-1}{2}} & m_p c^2 \ll T. \end{cases} \quad (2)$$

In particular, the ratio reaches its maximum value, $(m_p/m_e)^{(q-1)/2}$ (for $q > 1$), over most of the range of particle energies.

Similarly, the proton to electron energy density ratio

$$\kappa \equiv \frac{U_p}{U_e} = \frac{\int_{T_0}^{\infty} N_p(T) T dT}{\int_{T_0}^{\infty} N_e(T) T dT}, \quad (3)$$

can be expressed in terms of the spectral index q ,

$$\kappa(q) = \frac{\left[\frac{T_0^2}{c^2} + 2T_0 m_p\right]^{\frac{q-1}{2}} \int_{T_0}^{\infty} T(T + m_p c^2) \left[\frac{T^2}{c^2} + 2T m_p\right]^{-\frac{q+1}{2}} dT}{\left[\frac{T_0^2}{c^2} + 2T_0 m_e\right]^{\frac{q-1}{2}} \int_{T_0}^{\infty} T(T + m_e c^2) \left[\frac{T^2}{c^2} + 2T m_e\right]^{-\frac{q+1}{2}} dT}. \quad (4)$$

For example, if $q=2.5$, then $U_p/U_e \lesssim 10$, and $N_p/N_e \sim 1.3 \times 10^2$ at $T = 1$ GeV.

The spectrum of relativistic electrons is obviously more easily measured due to their much more efficient radiative losses. Most readily observed is electron synchrotron radio emission, which we will use to infer $N_e(\gamma)$ in the region where the radio emission is observed. To relate this quantity to the source spectrum we need to solve the kinetic equation describing the propagation mode and energy losses incurred by electrons as they move out from their SN shock regions. Using the above predicted proton to electron ratio at their common source region, and accounting for proton propagation mode and energy losses, we can then deduce the proton spectrum from the electron spectrum. Clearly, even if the propagation modes of protons to electrons are similar, their losses are very different; thus, N_p should be inferred from particle number conservation.

2.2. Steady State Particle Spectra

The enhanced SF activity in a starburst galaxy lasts for $O(10^8)$ yr, which is also the timescale over which global SN shock acceleration is prevalent. Estimated times for propagation out of the disk and inner galactic halo are about an order of magnitude lower for low energy particles. High energy particles lose energy on much shorter timescales. Thus, particle spectra evolve considerably as they propagate out of their acceleration sites. As long as typical acceleration times are comparable to or shorter than loss times for sufficiently high energies, a steady state can be attained, with particle spectra which are obviously steeper than their respective source spectra. Strictly speaking, we assume that steady state is attained and proceed to solve the kinetic equation for $N_i(\gamma, R, z)$, where R and z are the 2D spatial radius and the coordinate perpendicular to the galactic plane, respectively.

A full calculation of the particle steady state spectra is necessarily extensive as it must include all the important energy loss mechanisms and modes of propagation. We have employed the numerical code of Arieli & Rephaeli (Arieli & Rephaeli, in preparation), which is based on a modified version of the GALPROP code (Moskalenko & Strong 1998, Moskalenko et al. 2003), that has been developed for this purpose. The code solves the exact Fokker-Planck transport diffusion-convection equation (e.g., Lerche & Schlickeiser 1982) in 3D with given source distributions and boundary conditions for electrons and

protons. Evolution of the particle energy and spatial distribution function is based on diffusion, and convection by galactic wind. (We note that some of the additional processes included in the original code, such as diffusive re-acceleration, nuclear fragmentation, and radioactive decay, are not relevant for our purposes here.) Logarithmic coordinates are used for high spatial resolution.

The main focus of this first phase of our work is the estimation of the high energy flux of M 82. An approximate estimate of the high energy γ -ray emission can be obtained by a simple and intuitive calculation that is based on sampling the electron energy spectrum from the main observable – the radio synchrotron flux. However, because the electron spectrum needs to be extrapolated to energies much higher than the $\sim 1 - 10$ GeV range directly inferred from radio measurements, realistic estimates of the TeV emission necessitates a detailed (numerical) treatment. To illustrate this, and to provide insight on the results from the more accurate numerical calculation, we first outline the intuitive calculation.

2.3. Energy Loss Processes

At energies below few hundred MeV, electrons lose energy mostly by Coulomb interactions with gas particles, leading to ionization of neutral and charged ions, and electronic excitations in fully ionized gas. At higher energies the dominant energy losses are via synchrotron emission, and Compton scattering by the far-IR (FIR) and optical radiation fields. These well known processes need no elaboration; the level of the ensuing emission depends on the mean strength of the magnetic field, B , and the energy density of the radiation fields, which are specified below.

2.3.1. Gauging particle spectra by radio emission

The electron population consists mostly of directly accelerated (primary) electrons, which can be represented by a single power-law (in terms of the Lorentz factor)

$$N_e(\gamma) = N_{e,0} \gamma^{-q} \quad (5)$$

for $\gamma_1 \leq \gamma \leq \gamma_2$. The electron synchrotron flux from a region of radius r_s with magnetic field B , located at a distance d , is

$$f_\nu = 5.67 \times 10^{-22} \frac{r_s^3}{d^2} N_{e,0} a(q) B^{\frac{q+1}{2}} \times \left(\frac{\nu}{4 \times 10^6} \right)^{-\frac{q-1}{2}} \text{ erg}/(\text{s cm}^2 \text{ Hz}) \quad (6)$$

where $a(q)$ is defined and tabulated in, e.g., Tucker (1975).

Setting $\nu=1$ GHz and $\psi \equiv \left(\frac{r_s}{0.1 \text{ kpc}} \right)^{-3} \left(\frac{d}{\text{Mpc}} \right)^2 \left(\frac{f_{1 \text{ GHz}}}{\text{Jy}} \right)$, from Eq.(6) the normalization of the electron spectrum is

$$N_{e,0} = 5.72 \times 10^{-15} \psi a(q)^{-1} B^{-\frac{q+1}{2}} 250^{\frac{q-1}{2}} \quad (7)$$

A second relation is required to separately estimate N_e and B . This is provided by assuming that the energy density is equipartitioned between particles (electrons and protons) and the magnetic field,

$$U_p + U_e \simeq \frac{B^2}{8\pi} \quad (8)$$

The electron energy density is $U_e = N_{e,0} m_e c^2 \int_{\gamma_1}^{\gamma_2} \gamma^{1-q} d\gamma$, where $\gamma_1 \simeq 100$ corresponds to the energy below which Coulomb losses exceed synchrotron losses (the detailed number depends on the ambient, mostly thermal, density and magnetic field; e.g., Rephaeli 1979). For $q > 2$ and $\gamma_2 \gg \gamma_1$, we get $U_e \simeq N_{e,0} m_e c^2 \gamma_1^{2-q} / (q-2)$. Substituting the expression for $N_{e,0}$ from Eq.(7), we have

$$U_e U_e = 2.96 \times 10^{-22} 250^{\frac{q}{2}} \psi \frac{\gamma_1^{-q+2}}{(q-2)a(q)} B^{-\frac{q+1}{2}}. \quad (9)$$

Equation (9), together with Eqs.(3) and (8), then lead to

$$B_{\text{eq}} = \left[7.46 \times 10^{-17} \frac{(2.5 \times 10^{-2})^{q/2}}{q-2} \psi \frac{1 + \kappa(q)}{a(q)} \right]^{\frac{2}{5+q}} \quad (10)$$

From the above relations it can be readily seen that if the flux, source size, distance, and the spectral index of the emitting electron population (q) are known, then the source magnetic field – and hence the particle energy density – can be evaluated. For example, if $q=2.5$ (which corresponds to a typical galactic radio spectral index of 0.75) and $\psi = 1$, we obtain $B_{\text{eq}} \sim 65 \mu\text{G}$, $U_e \sim 9.5 \text{ eV cm}^{-3}$, $U_p \sim 95 \text{ eV cm}^{-3}$, $N_{e,0} \sim 9.2 \times 10^{-5} \text{ cm}^{-3}$.

2.3.2. FIR radiation field

In intensely star-forming regions the stellar IMF is top-heavy (e.g., Mayya et al. 2007), so massive stars are proportionally more abundant there than in more typical Galactic environments. During most of their lifetimes massive stars are embedded in the dense, highly extinguished regions (giant molecular clouds) where they were born (e.g., Silva et al. 1998). The radiation emitted by these stars peaks in the UV, which is very efficiently absorbed by the embedding dusty clouds and is re-emitted in the FIR. Therefore the local radiation field is most intense in the FIR region, where it can be described as an isotropic, diluted, modified blackbody with temperature T_d and spatial dilution factor C_{dil} :

$$n_{\text{FIR}} = C_{\text{dil}} \frac{1}{\pi^2 (\hbar c)^3} \frac{\epsilon^2}{e^{\epsilon/kT_d} - 1} \left(\frac{\epsilon}{\epsilon_0} \right)^\sigma \quad (11)$$

with $0 \leq \sigma \leq 2$, for which we choose $\sigma=1$ (e.g., Goldshmidt & Rephaeli 1995), and ϵ_0 corresponding to $\nu=2 \times 10^{12}$ Hz (Yun & Carilli 2002, and references therein). For a given T_d , the energy density of the warm dust, $U_{\text{FIR}}(C_{\text{dil}})$, can then be computed; comparison with the observed value, $U_{\text{FIR}}^{\text{obs}} = L_{\text{FIR}}^{\text{obs}} / (\pi r_s^2 c)$, where r_s is the radius of the accelerating source, yields C_{dil} .

When electrons whose energy distribution is as in Eq.(5) interact with this FIR radiation, the spectral emissivity of the isotropically Compton-scattered radiation is (e.g., Rybicki & Lightman 1979)

$$j_C(\epsilon) = C_{\text{dil}} F(q) \frac{N_{0,e} (e^2/mc^2)}{\pi^2 \hbar^3 c^2} (kT_d)^{\frac{q+5}{2}} \epsilon^{-\frac{q-1}{2}} \quad (12)$$

where $F(q) \equiv \frac{q^2 + 4q + 11}{(q+3)^2 (q+5)(q+1)} \Gamma\left(\frac{q+5}{2}\right) \zeta\left(\frac{q+5}{2}\right)$, with Γ and ζ denoting the Gamma function and the Riemann zeta function. For GeV electrons and typical dust temperatures, most of the emission is in the X-ray region.

2.3.3. γ -ray emission from π^0 decay

Proton energy losses at low energies are also dominated by Coulomb interactions with gas particles. At energies above pion masses (~ 140 MeV), the main energy-loss process is by interactions with ambient protons; the yield from this process are neutral (π^0) and charged (π^\pm) pions. Neutral pions decay into photons, while the decays of π^\pm yield relativistic positrons and neutrinos

The integral spectral emissivity from π^0 decay is:

$$g_\eta(\geq 1 \text{ TeV}) = g_\eta \left(\frac{\epsilon}{\text{TeV}} \right)^{3-\eta} \frac{\text{erg}}{\text{cm}^3} \text{s}^{-1} (\text{H atom})^{-1} \quad (13)$$

(Drury et al. 1994), where $\eta=q+2$. This emissivity is very strongly dependent on the proton power-law index; e.g., for momentum distribution indices $\eta=4.1, 4.3, 4.5, 4.7$, we deduce (using tabulated values from Drury et al. 1994) that the >100 GeV emissivity, $g(\geq 100 \text{ GeV})$ equals $1.28 \times 10^{-16}, 4.19 \times 10^{-17}, 9.49 \times 10^{-18}, 1.85 \times 10^{-18}$ erg $\text{cm}^{-3} \text{s}^{-1} (\text{H atom})^{-1}$, respectively.

The integrated γ -ray photon luminosity of a source with gas density n and proton energy density U_p in a volume V is then

$$L(\geq \epsilon) = \int_V g(\geq \epsilon) n U_p dV \text{ s}^{-1} \quad (14)$$

where both $g(\geq \epsilon)$ and U_p depend on the relativistic protons' spectral slope, q .

3. VHE emission from M 82: approximate treatment

In this section we estimate the level of VHE emission from hadronic interactions in M 82, the most prominent nearby ($d = 3.6$ Mpc) starburst galaxy. The radio emission of M 82 is observed to be power-law from $\nu_{\text{min}}=22.25$ MHz to $\nu_{\text{max}}=41$ GHz with a flux of 10 Jy at 1 GHz, and the spectrum steepening from $\alpha \simeq 0.71$ (Carlstrom & Kronberg 1991) in the central starburst ($r_s=300$ pc; e.g., Völk et al. 1996, Mayya et al. 2006) to $\alpha \simeq 1$ (Klein et al. 1988, Seaquist & Odegard 1990) in the outer disk. The high-frequency radio data from the central disk region are shown in Figure 1. While there is some curvature in the radio spectrum, because we are mostly interested here in the high-energy end of the electron spectrum, this curvature is ignored and we fit the spectrum by a single power-law model. We infer that the synchrotron radio emission is from a population of relativistic electrons whose energy spectrum – in the region sampled by the observed radio emission – is a power-law with index $q \simeq 2.42$.

Using the implied value of q , from Eqs.(2) and (4) we obtain $\kappa \simeq 10$ and $N_p/N_e|_{1 \text{ GeV}} \simeq 1.3 \times 10^2$. Estimates of the Galactic values of these energy densities are $U_p \sim 0.3$ eV cm^{-3} and $U_e \sim 0.03$ eV cm^{-3} , hence $\kappa \sim 10$ (see Schlickeiser 2002), and $N_p/N_e \sim 10^2$ at 1 GeV. The values of the two ratios are then quite similar in the two galaxies, in spite of their very different environments.

This similarity can be understood by the following argument. Typical SNR ages (hence, the duration of the acceleration processes), $\tau_{\text{SNR}} \lesssim 2 \times 10^4$ yr, are much shorter than the

characteristic energy-loss timescales of both electrons and protons in the remnant (even for the strongest magnetic fields in SNRs allowed by current IACT data, $B = O(10^2) \mu\text{G}$; e.g., Berezhko & Völk 2006), $\tau_s \sim 1$ Gyr and 0.5 Myr for GeV protons and electrons, respectively. Because of this, and the scaling of acceleration processes and propagation by rigidity, protons and electrons in the central disk region are expected to retain approximate similarity of their spectra at low to moderate energies (which dominate the particle distributions). Thus, the spectra have roughly the same spectral index both at injection ($q_i \simeq 2$) and, after injection, while diffusing in the central disk with a diffusion coefficient $\propto p^b$ with $b \sim 0.5$ ($q = q_i + b \sim 2.5$) (e.g., Büsching et al. 2001). This will hold both in the very actively star-forming central region of M 82 and in the relatively quiescent Galactic environment.

Using $q=2.42$, Eqs.(10), (7), and (9) along with $\kappa \equiv U_p/U_e \simeq 10$, and the above-quoted parameters appropriate for M 82, we derive: $B \simeq 95 \mu\text{G}$, $N_{e,0} \simeq 10^{-4} \text{ cm}^{-3}$, $U_e \simeq 20$ eV cm^{-3} , and $U_p \simeq 200$ eV cm^{-3} .

3.1. X-ray emission

Nonthermal X-ray emission is mostly by Compton scattering of the electrons by the FIR radiation field. To estimate the level of this emission, we first determine the energy density of the FIR field, whose dilution constant, C_{dil} , which appears in Eq.(11), is evaluated as follows. Using $T_d=45$ °K (Carlstrom & Kronberg 1991) in Eq.(11), the warm dust energy density is $U_{\text{FIR}}=5.55 C_{\text{dil}} 10^{-8}$ erg cm^{-3} . On the other hand, the measured flux is $f_{\text{FIR}} \simeq 6.5 \times 10^{-8}$ erg $\text{cm}^{-2} \text{s}^{-1}$, so that the observationally deduced value is $U_{\text{FIR}}^{\text{obs}} = L_{\text{FIR}}^{\text{obs}} / (\pi r_s^2 c) \simeq 1.26 \times 10^{-9}$. Equating U_{IR} to $U_{\text{FIR}}^{\text{obs}}$ yields $C_{\text{dil}}=0.023$. (This value is slightly reduced if one corrects the observed FIR luminosity of M 82 for cirrus emission.)

From Eq.(12) the differential Compton flux from the central SB of M 82 is $f_C(\epsilon) \simeq 4 \times 10^{-13} \epsilon^{-0.71}$ erg $\text{cm}^{-2} \text{s}^{-1} \text{keV}^{-1}$.

The emission is clearly in the X-ray range; e.g., electrons with γ as low as 150 and 350 boost a $60 \mu\text{m}$ photon (representative of the FIR field) to, respectively, 2 keV and 10 keV. Given their steep energy distribution, only electrons of relatively low energy will be effective in generating a substantial Compton flux. Thus, electrons with $100 \leq \gamma \leq 1000$ scattering off the 45 °K blackbody photons will boost their energies mostly to the 0.4-80 keV band. In particular, the predicted 2-10 keV Compton flux is $f_C(2 - 10 \text{ keV}) \simeq 10^{-12}$ erg $\text{cm}^{-2} \text{s}^{-1}$.

There is yet no unequivocal evidence for nonthermal X-ray emission in M 82. *Chandra* observations show that some of the 2-10 keV emission in M 82 is diffuse, emanating from a region which roughly overlaps with the central starburst (Griffiths et al. 2000). The 2-10 flux of this diffuse emission is 1.4×10^{-12} erg s^{-1} , some 5% of the total measured 2-10 keV emission (e.g., Cappi et al. 1999; Rephaeli & Gruber 2002). Given that some of this diffuse component may be thermal, as suggested by the presence of a substantial 6.7 keV Fe-K emission, the observed diffuse emission is a strong upper limit on our predicted lower Compton contribution.

3.2. VHE γ -rays

The value $q=2.4$ corresponds to $\eta=4.4$, for which we determine the appropriate value of g from Table 1 of Drury et al. (1994), and obtain $g(\geq \epsilon)=8.1 \times 10^{-19}(\epsilon/\text{TeV})^{-1.4} \text{ erg}^{-1} \text{ cm}^3 \text{ s}^{-1} \text{ atom}^{-1}$, which holds approximately down to ~ 10 GeV (e.g., Torres 2004; Domingo-Santamaría 2006).

A rough estimate of the VHE emission from M 82 can be made if it assumed that this emission comes mostly from π^0 decay following interactions of energetic protons with ambient protons in the central disk. In this approximate treatment we also ignore contribution to the VHE emission by electron radiative processes. Assuming that acceleration only occurs in the central SB (of radius r_s), we thus take the proton energy density to be $U_p(R) \sim 200(R/r_s)^{-2} \text{ eV cm}^{-3}$ for $R > r_s$, and consider separately the emission from the central SB and disk regions:

(i) In the central SB region ($R \leq r_s$) the hydrogen mass is mostly molecular, $M_{\text{H}_2} \simeq 2 \times 10^8 M_\odot$ (Weiss et al. 2001). The estimated VHE photon luminosity is then $L(\geq 100 \text{ GeV}) \simeq 1.6 \times 10^{39} \text{ s}^{-1}$.

(ii) The disk region external to the central SB, $R > r_s$, has a flat thin disk gas distribution, $\Sigma(R) = \Sigma(0) e^{-R/R_D}$, with $\Sigma(0) \simeq 7.5 \times 10^{22} \text{ cm}^{-2}$ the effective central density and $R_D \sim 0.82 \text{ kpc}$, the radial lengthscale (Mayya et al. 2006). The total gas mass, $M_{\text{gas}} \simeq 2.5 \times 10^9 M_\odot$, results from $M_{\text{HI}} \simeq 7 \times 10^8 M_\odot$ and $M_{\text{H}_2} \simeq 1.8 \times 10^9 M_\odot$ (Casasola et al. 2004). The energetic proton energy density is assumed to have the form $U_p(R) = 200 (R/r_s)^{-2} \text{ eV cm}^{-3}$. From

$$L(\geq \epsilon) \simeq 2\pi R_D^2 U_p \sigma_{\text{gas}}(0) g(\geq \epsilon) \int_{0.366}^{\infty} \frac{e^{-x}}{x} dx \text{ s}^{-1},$$

we then obtain $L(\geq 100 \text{ GeV}) \simeq 1.5 \times 10^{40} \text{ s}^{-1}$.

The resulting total photon luminosity, $\simeq 1.7 \times 10^{40} \text{ s}^{-1}$, translates into a flux $f(\geq 100 \text{ GeV}) \simeq 1.1 \times 10^{-11} \text{ cm}^{-2} \text{ s}^{-1}$.

Before accepting the above estimate as physically meaningful, we need to ascertain that energetic protons do indeed leave their SN acceleration sites, and that VHE photons propagate freely through the galactic disk. Indeed, even in large, $R \sim 10$ pc, dense molecular clouds with typical ambient proton density of order 10^2 cm^{-3} , the optical depth to pp interactions is very low, $\tau_{\text{pp}} \sim \sigma_{\text{pp}} n_p l \sim 3 \times 10^{-4}$, where the cross section for pp interactions is $\sigma_{\text{pp}} \sim 10^2 \text{ mb} = 10^{-25} \text{ cm}^2$ (e.g., Eidelman et al. 2004). This estimate is in obvious agreement with the fact that energetic protons at the relevant energy range are actually detected on Earth.

Absorption of VHE photons is also negligible; the optical depth to pair production by interactions with ambient photons, $\tau_{\gamma\gamma} = n_\gamma \sigma_{\gamma\gamma} l$ (where n_γ is the target photon number density, $\sigma_{\gamma\gamma}$ is the $\gamma\gamma$ cross section, and l is the distance traveled), is also very small. For TeV photons, the peak cross section, $\sigma_{\gamma\gamma} = 1.7 \times 10^{-25} \text{ cm}^2$, is for interaction with $\sim 2 \mu\text{m}$ photons. The $2 \mu\text{m}$ luminosity, $L_{2\mu\text{m}} = 2 \times 10^{43} \text{ erg s}^{-1}$ (e.g., Silva et al. 1998), implies a $2 \mu\text{m}$ photon density of $\sim 0.5 \text{ cm}^{-3}$ (assuming a disk radius $r_{\text{gal}} \sim 7 \text{ kpc}$), i.e. $\tau_{\gamma\gamma} \sim 10^{-3}$. We conclude that absorption of VHE photons in – and indeed also along the l.o.s. to – M 82 is negligible.

4. Particle and Radiation Spectra in M 82: Full Numerical Treatment

As specified above, the central SB region, with a radius of 300 pc and height of 200 pc (e.g., Volk et al. 1996), is identified as the main site of particle acceleration. The superposed particle spectra from all SN shock regions yields the power-law distributions with index $q=2$ (as mentioned in section 2). The theoretically predicted N_p/N_e ratio (e.g., Schlickeiser 2002) is more likely to be valid in this source region, as is also the assumption of equipartition. Accordingly, we infer N_p in the source region from N_e , which itself is deduced from radio measurements in the central disk, as explained below.

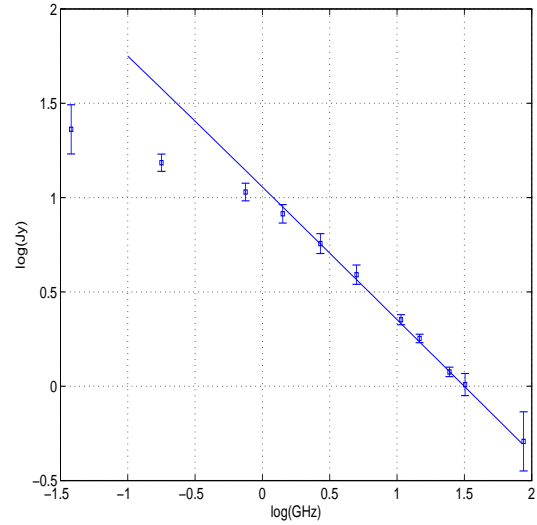


Fig. 1. Radio measurements (from Klein et al. 1988) and best-fit power-law spectrum to the data above 0.75 GHz.

Particles are assumed to be convected out of their sources by the observed wind with velocity of 600 km s^{-1} (Strickland et al. 1997). The convection velocity is assumed to increase linearly with distance from the disk plane. This assumption is consistent with cosmic-ray MHD wind models (e.g. Zirakashvili et al. 1996). The diffusion coefficient is taken as a power-law in rigidity $D_{xx} \propto (\rho/\rho_0)^\delta$, where ρ_0 is a scale rigidity with a typical index of 0.5. Particle energy losses and propagation outside the source region are followed in detail using the code of Arieli & Rephaeli. To do so we need the neutral and ionized gas densities and their profile, as well as the spatial variation of the mean strength of the magnetic field.

We use the neutral, molecular, ionized gas, and FIR radiation field parameters specified above. Additionally, we assume magnetic flux freezing in the (highly conductive) ionized gas, so that the local magnetic field strength is related to the ionized gas density, n_{HII} , using the scaling $B \propto n_{\text{HII}}^{2/3}$ (e.g., Rephaeli 1988). Measurements of radio emission from the central disk (Klein et al. 1988), shown in Figure 1 together with our best fit power-law with index of 0.71 ± 0.02 (which is consistent with the results of Klein et al. 1988, and Carlstrom et al. 1993), provide the first relation between the electron density in this region and the magnetic field. Note that we ignore here the flattening

indicated in the radio spectrum at $\nu \leq 300$ MHz (which is possibly due to the increased relative strength of Coulomb losses at low electron energies) since we are primarily interested in the high energy behavior of the electron spectrum. The second required condition to fully determine particle spectra and the magnetic field is the assumption of equipartition in the source region. Due to the implicit dependences in the expression for the synchrotron flux, this condition is implemented iteratively to solve for N_e , N_p , and B_0 . With the above parameters the central value of the magnetic field is $B_0 \simeq 310 \mu\text{G}$. An index of ~ 0.7 implies that the electron spectrum in the central disk steepens appreciably (near ~ 1 GeV) to $q_{\text{cd}} \sim 2.4$ from its value (2) in the source region. The steady-state electron and proton spectra in the central disk region are shown in Figure 2. At low energies the spectra are flat; stronger losses at high ($E \gg 1$ GeV) energies result in a steeper spectrum than that of protons, with the electron spectrum characterized by $q_{\text{cd}} \sim 2.6$ at very high energies.

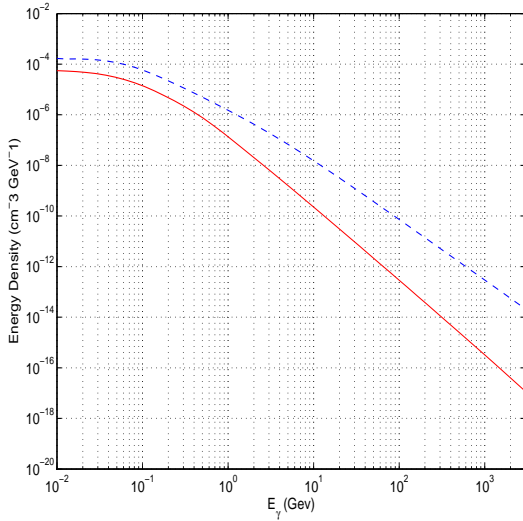


Fig. 2. Steady state primary electron (solid line) and proton (dashed line) spectral density distributions in the central disk region.

Electron emissions by bremsstrahlung and Compton scattering are shown in Figure 3; also shown is γ -ray emission from π^0 decay (following p-p collisions). As expected, the losses due to bremsstrahlung dominate the lower energy regime, whereas losses due to π^0 decay dominate at higher energies. (While synchrotron emission extends to the X-ray region, it is negligible at much higher energies.) Our main interest here is the VHE emission, which – as anticipated – is mainly from the latter process. Specifically, we calculate a total flux from the galactic disk to be $f(\geq 100 \text{ GeV}) \simeq 3.5 \times 10^{-12} \text{ cm}^{-2} \text{ s}^{-1}$; the flux at $\epsilon \geq 50 \text{ GeV}$ is a factor of ~ 3 higher.

While we are mostly interested here in the VHE photon emission, we note that the related neutrino flux (from $\pi^+ \rightarrow \mu^+ + \nu_\mu \rightarrow e^+ + \nu_e + \bar{\nu}_\mu + \nu_\mu$) at energies higher than 100 GeV is $\sim 0.3 f(\geq 100 \text{ GeV})$.

These predicted fluxes are roughly a factor of ~ 3 lower than those estimated in the approximate calculation. Given the

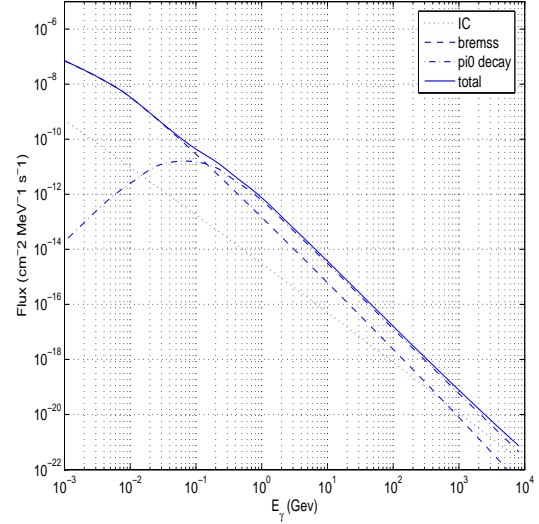


Fig. 3. Shown are emission spectra from the central disk region of M 82. Radiative yields are from electron Compton scattering off the FIR radiation field (dotted line), electron bremsstrahlung off ambient protons (dashed line), π^0 decay following pp collisions (dashed-dotted line), and their sum (solid line).

nature of the approximations made, and the fact that spatial dependences of the particle densities and magnetic field were altogether ignored, this level of discrepancy is not surprising.

5. Discussion

Our main objective has been an improved estimate of the TeV emission from the nearby northern-sky starburst galaxy M 82. This has been obtained first by an approximate calculation of the hadronic emission alone, and then a more comprehensive and detailed treatment which follows the evolution of the steady state electron and proton spectra and their radiative yields, taking into account pertinent energy losses and propagation modes. (Note though that because TeV emission is largely produced in the central disk, details of our modeling of the diffusion coefficient and convection velocity are not that important in determining the particle spatial profile over this relatively small region.) Of course, only the full, more physically meaningful and realistic treatment provides a consistent basis for predicting the full particle and radiation spectra. The fact that we account for all known energy loss processes substantiates our expectation that the electron spectrum can be extrapolated to energies much higher than the range directly sampled by radio measurements. The approximate calculation is included here in order to give intuitive insight on the main contribution to the TeV emission, and in order to relate our work to previous similar treatments.

As we have already noted, the factor of ~ 3 discrepancy in our two estimates of the TeV flux is actually quite small, given the rough nature of the approximate calculation. This is so mainly due to the fact that we have focused here on the estimation of the VHE emission which is largely restricted to the relatively small central part of M 82. Over this region evolution

of the particle spectra is moderate. Moreover, most of the VHE emission is from π^0 decay, which does not require detailed calculation of the electron spectrum. Of course, the approximate calculation is totally inadequate in predicting the lower energy emission, especially so over the larger disk region.

Compared to previous estimates of γ -ray emission from M 82 (e.g., Akyüz et al. 1991; Pohl 1994; Völk et al. 1996), our detailed treatment is more realistic by virtue of being more tuned to a range of observables. These include the neutral and ionized gas densities and their estimated profiles across the central galactic disk, as well as the anticipated spatial variation of the magnetic field across this region. Most importantly, the basic normalization of the electron spectrum is directly determined from the measured radio spectrum. We assume equipartition and an initial, theoretically predicted N_p/N_e ratio only in the starburst source region, where these are more likely to be valid, rather than across the full disk as in previous work. Finally, we include all the dominant radiative electron and proton processes. The calculation of Torres (2004), who estimated emission from the super-starburst galaxy Arp 220, and those of Paglione et al. (1996) and Domingo-Santamaría & Torres (2005), who estimated VHE emission from the southern-sky starburst galaxy NGC 253, although similar are still appreciably different from our numerical treatment. Given the substantial differences between our approach and those adopted in most previous treatments, it is not very meaningful to carry out a more detailed comparison of specific differences – e.g., in parameter values and spatial profiles, including those of the electron and proton densities, and mean magnetic field in the central disk region – and we avoid doing so here.

An assessment is needed of the reliability of our basic result – the predicted level of TeV emission. Clearly, this flux depends linearly on N_p , which in turn is related to N_e . The electron density was deduced from the measured radio emission in the central disk region, which is not much larger than the particle SB source region. Therefore, the evolution of the electron spectrum from the latter region to the central disk region is mostly determined by synchrotron losses in the high magnetic field. From Eqs. (6) and (8) it follows that $N_p \propto B_{eq}^2$ (which is obvious in the limit $U_p \gg U_e$). The uncertainty in the estimated level of TeV emission stems mostly from this steep dependence. It is unlikely that the field is appreciably higher than our estimate ($B_0 \simeq 310 \mu\text{G}$), but it could possibly be lower. For example, a value lower by a factor of ζ , would reduce N_p and π^0 decays by a factor ζ^2 . However, for a given measured radio flux N_e would have to be higher by the factor $\zeta^{(1+q)/2}$, which for a mean electron index of ~ 2.4 (over the central disk) would result in a boost of the bremsstrahlung and Compton yields by nearly the same factor ($\sim \zeta^2$). As can be seen in Figure 3, in the TeV region, the yield from the latter processes is only a factor ~ 2 lower than emission from π^0 decay, implying, e.g., that if the field were reduced to $B_0 \simeq 200 \mu\text{G}$, the total TeV emission would hardly change at all. Thus, the net effect of a lower field strength on the TeV emission is very small. Of course, the π^0 decay yield is linearly dependent also on the ambient proton density, which we inferred directly from the measured mass in the central disk. We conclude that our predicted TeV flux is not likely to be appreciably over-estimated. [By a numerical coin-

idence in spite of the different approach, our (numerical) TeV flux estimate is very similar to that by Völk et al. 1996, which was assumed to be emitted from the central starburst only, and to be purely hadronic with a hard ($q=2.1$) proton population throughout the emission region.]

Based on the above estimate it seems that the predicted VHE of M 82 is below the detection limit of current imaging Cerenkov telescopes, such as MAGIC and VERITAS. For example, the MAGIC telescope – which is located in the Northern hemisphere and can therefore observe M 82 – has a 5σ sensitivity of $\sim 2 \times 10^{-11} \text{ cm}^{-2} \text{ s}^{-1}$ for the detection of emission above 100 GeV in ~ 50 hours of observation (Bastieri et al. 2005). However, this sensitivity limit was derived assuming a power-law source whose (photon) flux has an index of 2.6, somewhat steeper than the index we obtain in the TeV region, ~ 2.3 . Taking this into account yields a higher sensitivity by a factor of a few, which brings our estimated flux, $f(\geq 100 \text{ GeV}) \sim 3.5 \times 10^{-12} \text{ cm}^{-2} \text{ s}^{-1}$, within the detection threshold. We conclude that measurement of TeV emission from M 82, or obtaining an interesting upper limit on it, is feasible with MAGIC I. Prospects are even better with the factor $\lesssim 3$ improvement in sensitivity expected with the upcoming MAGIC II telescope.

References

- Akyüz, A., Brouillet, A., & Özel, M.E. 1991, *A&A*, 248, 419
 Bastieri, D., et al. 2005, *Astrop. Physics*, 23, 572
 Berezhko, E.G., & Völk, H.J. 2006, *A&A*, 451, 981
 Blandford, R.D., & Ostriker, J.P. 1978, *ApJ*, 221, L29
 Büsching, I., Pohl, M., & Schlickeiser, R. 2001, *A&A*, 377, 1056
 Casasola, V., Bettoni, D., & Galletta, G. 2004, *A&A*, 422, 941
 Cappi, M., Persic, M., Bassani, L., et al. 1999, *A&A*, 350, 777
 Carlstrom, J.E., & Kronberg, P.P. 1991, *ApJ*, 366, 422
 Domingo-Santamaría, E. 2006, PhD thesis (Universidad Autónoma de Barcelona)
 Domingo-Santamaría, E., & Torres, D.F. 2005, *A&A*, 444, 403
 Drury, L.O’C., Aharonian, F.A., & Völk, H.J. 1994, *A&A*, 287, 959
 Goldshmidt, O., & Rephaeli, Y. 2005, *ApJ*, 444, 113
 Eidelman, S., et al. 2004, *Phys Lett B*, 592, 1 (see <http://pdg.lbl.gov>)
 Freedman, W.L., et al. 1994, *ApJ*, 427, 628
 Griffiths, R.E., Ptak, A., Feigelson, E.D., et al. 2000, *Science*, 290, 1325
 Klein, U., Wielebinski, R., & Morsi, H.W. 1988, *A&A*, 190, 41
 Lerche, I., & Schlickeiser, R. 1982, *MNRAS*, 201, 1041
 Mayya, Y.D., Bressan, A., Carrasco, L., & Hernandez-Martinez, L. 2006, *ApJ*, 649, 172
 Paglione, T.A.D., Marscher, A.P., Jackson, J.M., & Bertsch, D.L. 1996, *ApJ*, 460, 295
 Moskalenko I.V., & Strong A.W. 1998, *ApJ*, 493, 694
 Moskalenko I.V., Jones, F.C., Mashnik, S.G., Ptuskin, V.S., & Strong A.W., 2003, *ICRC*, 4, 1925
 Persic, M., & De Angelis, A. 2008, *A&A*, in press (arXiv:0711.2317)
 Persic, M., & Rephaeli, Y. 2007, *A&A*, 463, 481
 Pohl, M. 1994, *A&A*, 287, 453
 Protheroe, R.J., & Clay, R.W. 2004, *PASA*, 21, 1
 Rephaeli, Y. 1979, *ApJ*, 227, 364
 Rephaeli, Y. 1988, *Comm. Ap.*, 12, 265

- Raphaeli, Y., & Gruber, D. 2002, *A&A*, 389, 752
- Rybicki, G.B., & Lightman, A.P. 1979, *Radiative Processes in Astrophysics*, p.202–208
- Rieke, G.H., et al. 1980, *ApJ*, 238, 24
- Schlickeiser, R. 2002, *Cosmic Ray Astrophysics* (Berlin: Springer), p.472
- Seaquist, E.R., & Odegard, N. 1991, *ApJ*, 369, 320
- Silva, L., et al. 1998, *ApJ*, 509, 103
- Strickland, D.K., Ponman, T.J., & Stevens, I.R. 1997, *A&A*, 320, 378
- Thompson, T.A., Quataert, E., & Waxman, E. 2007, *ApJ*, 654, 219
- Torres, D.F. 2004, *ApJ*, 617, 966
- Tucker, W. 1975, *Radiation Processes in Astrophysics* (Cambridge, MA: MIT Press)
- Yun, M.S., & Carilli, C.L. 2002, *ApJ*, 568, 88
- Völk, H.J., Aharonian, F.A., & Breitschwerdt, D. 1996, *SSRv*, 75, 279
- Völk, H.J., Klein, U., & Wielebinski, R. 1989, *A&A*, 213, L12
- Weiss, A., Neinger, N., Hüttemeister, S., & Klein, U. 2001, *A&A*, 365, 571
- Zirakashvili, V.N., Breitschwerdt, D., Ptuskin, V.S., & Voelk, H.J. 1996, *A&A*, 311, 113